Experimental Study of Self-starting Characteristics for H-Type Wind Turbine

J. Y. Zhu[1,2†] and P. Q. Liu[1]

[1] *Key Laboratory of Fluid Mechanics, Ministry of Education, Beihang University, Beijing, 100083, China*
[2] *College of Aeroengine, Shenyang Aerospace University, Shenyang, Liaoning Province, 110136, China*

†*Corresponding Author Email: michellend@126.com*

ABSTRACT

In order to study self-starting characteristics for H-type wind turbine, firstly, the effect of low Reynolds number and large separated flow on aerodynamic characteristics of airfoil were analyzed in detail, then two H-type wind turbines with different aerodynamic configurations were tested in a low speed wind tunnel for collecting the static torques at different phase angles and time-rotating speed curves in starting process. Based on theoretical analysis and experimental data, the cause of self-stating problem of H-type wind turbine has been revealed. The aerodynamic profile parameters of the wind turbine are closely related to the dependency of starting on initial phase position, and the minimum static torque determines whether the wind turbine has potential to start from rest. The time-rotating speed curves exhibit two different starting behaviour features, determined by the minimum dynamic torque in driving force conversion stage. Unless both the minimum static torque and minimum dynamic torque in driving force conversion stage are greater than the friction torque, the self-starting of the wind turbine cannot be realized. The typical self-starting behavior characteristics is that the time-rotating speed curve includes four different stages of initial linear acceleration, plateau, rapid acceleration and stable equilibrium with the final tip speed ratio more than 1.

Keywords: Wind energy; H-type wind turbine; Self-starting; Aerodynamic characteristics; Wind tunnel test.

1. INTRODUCTION

The Darrieus wind turbine is the typical vertical axis lift type wind turbine, the H-type wind turbine with multiple straight blades rotating around the rotating axis is the common type. The advantages of H-type wind turbine are its simple structure, no need for tracking wind devices, and low aerodynamic noise (Bhutta *et al*. 2012; Zhu *et al*. 2017). Compared to the horizontal axis wind turbine, the H-type wind turbine has high utilization efficiency of wind energy in complex wind fields such as high wind speed, high turbulence level, and cross winds. Therefore, the small H-type wind turbine is suitable for distributed power generation system in urban wind environment, where the energy is most needed (Li *et al*. 2013). However, due to lack of starting assist, the starting of H-type wind turbine only relies on the aerodynamic torque generated by its own blades (Singh *et al*. 2012). The self-starting problem has limited the widespread use of H-type wind turbine.

Current research on the aerodynamic characteristics of the H-type wind turbine focuses mostly on improving the wind energy utilization efficiency, ignoring the starting performance. Improving the starting performance of the wind turbine helps to shorten the starting time of the wind turbine and extend the power generation time, which in turn improves the overall efficiency. Firstly, it is needed to define the concept of "self-starting". Kirke (1998) considered that "self-starting was a process in which the wind turbine accelerated from rest to the significant power output". However, there was no explicit expression of "load" and "significant power output". Lunt (2005) proposed a clear definition and pointed out that "the wind turbine accelerated from rest until it reached a steady state with the tip speed ratio more than 1". The Lunt's definition was based on the pure aerodynamic characteristics and the fact that when the tip speed ratio exceeded 1, the wind turbine relies entirely on significantly increased lift force. Worasinchai (2012) took into account the load, the aerodynamic shape of the wind turbine, the airfoil and other factors, and pointed out that the self-starting should be that the wind turbine accelerated from rest,

meanwhile, the aerodynamic torque continuously outputs till the aerodynamic torque and the load were balanced. From the above different definitions, it can be seen that the self-starting performance is not only related to the aerodynamic characteristics of the wind turbine, but also generator load and other factors. Dominy *et al.* (2007) pointed out that only when these factors were understood individually could the wind turbine and its load be matched effectively.

From the aerodynamic viewpoint, there are still disputes whether the H-type wind turbine has self-starting capability. Kentfield (1996) pointed out that the H-type wind turbine was not capable of self-starting without auxiliary measures. The aerodynamic performance of the H-type wind turbine was theoretically analyzed by Biadgo *et al.* (2013). It was pointed out that the wind turbine with NACA0012 airfoil and the solidity of 0.15 produced negative torques at small tip speed ratios, which caused the wind turbine be not self-starting. Dominy *et al.* (2007) developed mathematical models to study the influence of the blades number on the starting behavior of H-type wind turbine with NACA0012 airfoil, the results showed that the three-blade wind turbine with light load had the potential of self-starting, while the starting of the two-blade wind turbine was related to the initial phase angle. Hill *et al.* (2009) conducted the wind tunnel experiment on a three NACA0018 blade H-type wind turbine with the solidity of 0.33 to obtain the time-rotating speed curve in the starting process at 6m/s and analyze the self-starting characteristics, and deemed the wind turbine to be self-starting. Chua (2002) tested a three NACA0015 blade H-type wind turbine and drawn the similar conclusions as Hill. The only two experiments conducted by Hill and Chua provide time-series behaviour, the limited test data prohibit the deep and systematic analysis on self-starting characteristics. Sengupta *et al.* (2016) experimentally studied the influence of airfoil on the starting time of H-type wind turbine. It was found that the EN0005 blade H-type wind turbine exhibited minimum starting time compared to the S815 and NACA0018 blade H-type wind turbines. However, the test lacks further analysis of the starting process. In recent years, Asr *et al.* (2016), Singh *et al.* (2015), Arab *et al.* (2017) and Zuo *et al.* (2014) verified the feasibility of the CFD numerical simulation method with the limited self-starting experimental data. The influence of airfoil, pitch angle, moment of inertia and other factors on the self-starting characteristics were analyzed . respectively.

In order to provide more experimental data for mathematical modelling and reliability verification of numerical method, and to further improve the understanding of self-starting characteristics, two H-type wind turbines with different aerodynamic configurations have been tested in the low speed wind tunnel. The static torques at different phase angles are measured and the starting behaviour in a time-history format is also acquired. Based on the experimental data, the cause of self-starting difficulty for H-type wind turbine has been revealed, and the criterion of self-starting has been further clarified.

2. THEORETICAL ANALYSIS

The design wind speed of small vertical axis wind turbine usually ranges from 4m/s to 15m/s, the chord length of the blade c is usually 0.2~0.3m. Therefore, the order of magnitudes of Reynolds number Re based on the blade chord length ($Re = \rho V_\infty c / \mu$, in which ρ is the density, μ is the dynamic viscosity coefficient) is limited to 10^5. The corresponding operating Reynolds number of the micro wind turbine will be much lower, falling into the category of typically low Reynolds number (Islam *et al.* 2008; Zhao *et al.* 2016) At low Reynolds number, the fluid flow in a laminar state with weak ability to resist inverse pressure gradient is easy to produce complex flow phenomenon such as laminar separation, transition and reattachment.

The object of study is H-type vertical axis wind turbine. Figure1 shows the diagram of phase position and clockwise rotation of the tested wind turbine. The incoming stream flows from left to right. The Eq. (1) and (2) are used to calculate the local angle of incidence α and tip speed ratio λ, respectively.

$$\alpha = \tan^{-1}(\frac{\sin \theta}{\lambda + \cos \theta}) \qquad (1)$$

$$\lambda = \omega R / V_\infty \qquad (2)$$

where θ is the phase angle, V_∞ is the wind speed, R is the rotation radius, ω is the angular velocity, and W is the resultant velocity of wind speed V_∞ and the rotation speed $R\omega$. The specific Darrieus movement makes α and W change periodically in the rotating process.
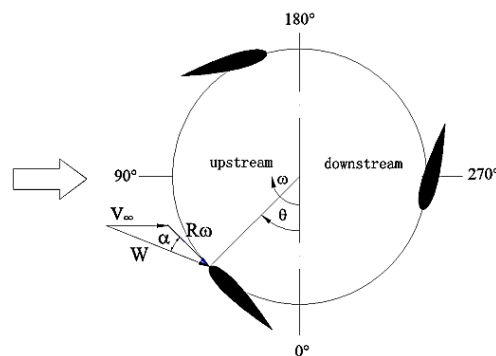
Fig. 1. Phase position and motion diagram of H-type wind turbine.

Figure 2 shows the curves of the angle of incidence with phase angle when the tip speed ratio λ is 0, 0.5 and 1, respectively. It can be seen that when the tip speed ratio λ is less than 1, the angle of

incidence curve is similar to the tangent curve, the corresponding angle of incidence ranges from -180° to 180°. Therefore, the wind turbine in the starting process suffers from separation flow with large angle of incidence. What is more, the gradually increased rotation speed in the starting process aggravates the unsteadiness of the resultant velocity, which makes the local Reynolds number of the blades change sharply.
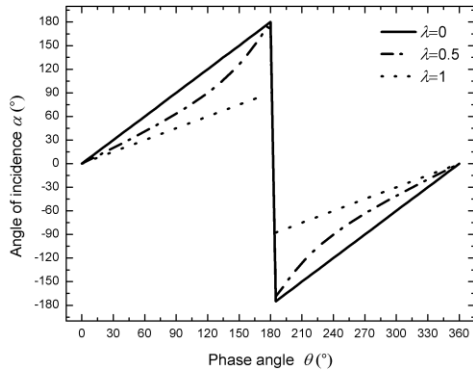
Fig. 2. Relation between angle of incidence and phase angle under different tip speed ratio.
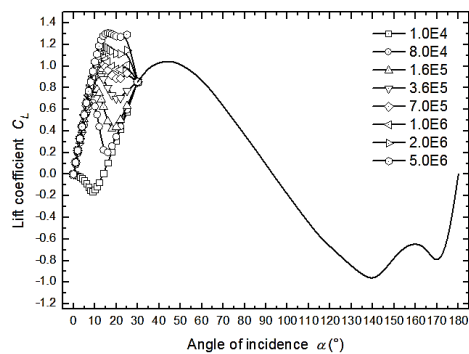
a. Lift coefficient
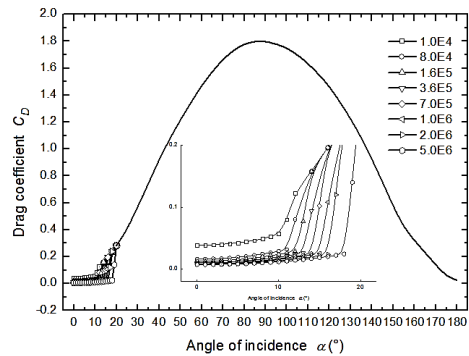
b. Drag coefficient

Fig. 3. Aerodynamic coefficient of NACA0018 airfoil (Sheldahl 1981).

Through the above analysis, the small H-type wind turbine suffers from the low Reynolds number and the large flow separation in the starting process that directly affects the lift-drag characteristics of the blade airfoil. Figure3 shows the lift coefficient and drag coefficient of NACA0018 airfoil at different Reynolds numbers (Sheldahl 1981). It can be seen that the maximum lift coefficient and the stall angle of incidence decrease sharply with the decrease of the Reynolds number, when the angle of incidence is less than 30°. At very low Reynolds number, the lift coefficient in the range of small angles of incidence particularly varied nonlinearly at Reynolds number of 10^4. The drag coefficient increases with the decrease of Reynolds number before the angle of incidence of 20°. The airfoil is in deep stall, acting like the plate at high angle of incidence, the lift coefficient and the drag coefficient of which are independent with Reynolds number. The aerodynamic data of airfoils is indispensable for theoretical analysis and results discussion, while the airfoil data at full angles of incidence with low Reynolds number is still limited, which prohibit the theoretical study of self-starting for H-type wind turbine.

3. EXPERIMENTAL METHODOLOGY

3.1 Test Model and Test Device

The test model is three-blade H-type wind turbine, of which the three blades are connected with the main shaft through the support arms with the pitch angle of 0°. The configuration parameters of two wind turbines are shown in Table 1. The solidity of the wind turbines are 0.409 and 0.454, respectively. Figure4 shows the wind turbine B installed in the wind tunnel test section.

Fig. 4. Wind turbine B test model.

Fig. 5. Low Speed Wind Tunnel.

Table 1 Aerodynamic shape parameters of the test wind turbines

	Blade airfoil	Chord length c/mm	Height H/mm	Rotating radius R/mm
Wind turbine A	NACA0012	90	500	330
Wind turbine B	NACA0018	100	600	330

The experiment was carried out in a low-speed and closed return wind tunnel located in Shenyang Aerospace University, which has the rectangular test section of 1.2m(W)×1.0m(H)×3m(L), as shown in Fig.5. The stably controllable wind speed ranges from 4m/s to 50m/s with the turbulence intensity less than 0.14%. The wind turbine model dimension will be too small if the blockage ratio meets the requirement of 10% in wind turbine experiment, which leads to very low Reynolds number different from that in actual operating condition. Furthermore, too small wind turbine produces relatively minor aerodynamic force, unfavourable for measurement. Given this article mainly focuses on the qualitative investigation of starting characteristics and aerodynamic force, rather than exact values free from wall interference. Therefore, the relatively larger wind turbines are chosen, the blocking ratios of wind turbine A and wind turbine B are 27.5% and 33%, respectively, which are relatively higher than the required blocking ratio.

3.2 Test Method

The study of the starting characteristics of the wind turbine mainly includes static torque characteristic and dynamic startup characteristic. The static torque distribution under different phase angles is used to evaluate whether the wind turbine has the potential for self-starting, and the process of accelerating from the rest to the maximum stable speed is used to evaluate whether the wind turbine can complete the whole process of self-starting.

The static torque test: the static torque of the H-type wind turbine is closely related to the phase position. The static torque is obtained by tension times arm length. The bottom end of the main shaft supporting the H-type wind rotor passes through the floor of the test section, and vertically links to the beam with a certain length. The tension is measured by a high-precision tension gauge with the range of 10N and the accuracy of 0.05N. Since the wind turbine has three blades, the static torque is one cycle at every 120° phase angle. Therefore, it is just a matter of measuring the static torque in one cycle, that is, at range of phase angle from 0° to 120°. In order to acquire relatively higher aerodynamic force to improve the accuracy, the test wind speed is selected to be greater than 10m/s.

The start acceleration test: the bottom end of the shaft links to rotation speed meter with the range of 6000rpm and the accuracy of ±0.1%, which is used

to collect the time-rotating speed data during the starting process with the sampling of 10Hz. In order to determine the minimum starting wind speed, the test wind speed gradually increases from the lowest stable wind speed that can be achieved by the wind tunnel until the wind turbine can start to rotate from rest. The minimum starting wind speeds are 12m/s and 8m/s for wind turbine A and wind turbine B, respectively. In the starting process, no extra load is applied on the shaft, except for the system friction torque less than 0.03Nm.

4. RESULTS AND DISCUSSIONS

4.1 Static Torque Characteristics

The static torque is transformed to the dimensionless form by Eq. (3), so that the static torque coefficient C_{st} is obtained, where T_s is the static torque and ρ is the air density.

$$C_{st} = T_s / (\rho V_\infty^2 HR^2) \tag{3}$$

Figure 6 shows the static torque coefficients with the phase angles of the wind turbine A and B under different wind speeds. As shown in Fig.6a, the wind turbine A has the positive torque value for most of the phase positions in one cycle except for range of $37.5° \le \theta \le 52.5°$. In addition, the local minimum static torque coefficients exist at $\theta = 0°$ and $\theta = 48°$, respectively, the former is positive, while the latter is negative. Especially the static toque coefficient goes from positive to negative around $\theta = 40°$, indicating that there exists "dead zone" of self-starting. Therefore, the wind turbine A does not have the ability to be self-starting. It can be seen that from Fig.6b, the static torque coefficients of the wind turbine B are always positive under all phase angles, indicating that, theoretically, the wind turbine B has the potential of self-starting. There exist the local minimum static torque coefficients at $\theta = 45°$ and $\theta = 75°$, respectively. If the minimum static torques are less than the friction torque, the wind turbine cannot start from the rest as well. From the static torque characteristics of these two wind turbines, not all three-blade H-type wind turbines are self-starting independent of phase position, and the airfoil and aerodynamic dimension used by the wind turbine play an important role.
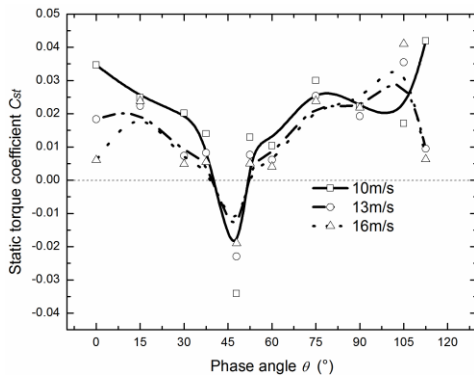
a. Wind turbine A
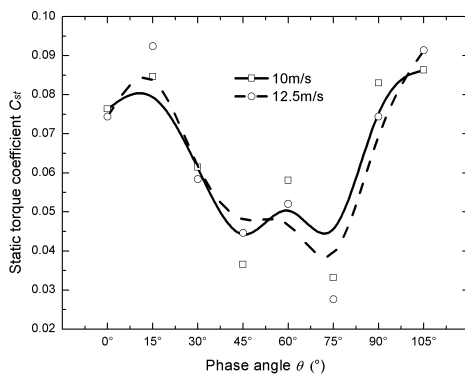
b. Wind turbine B

Fig. 6. Static torque coefficient distribution under different wind speeds.

Besides, the higher wind speed corresponds to the higher Reynolds number. It can be seen that from Fig.6a and 6b, as the Reynolds number increases, the static torque coefficients of both wind turbines decrease, as well as the static torque coefficient difference under different Reynolds number.

4.2 Starting Behavior Characteristics

The static torque characteristics can show "dead zone" of self-starting, thus judging whether the wind turbine has the potential of self-starting, that is, whether the wind turbine can start to rotate from the rest. However, it is necessary to monitor the he rotating speed with time during starting process and analyze the starting behaviour characteristics for judging whether the wind turbine can accelerate to working speed and realize the self-starting.

Figure 7a and 7b show the curves of the rotating speed with time of two wind turbines at different wind speeds, respectively. The wind turbine A can start, when the initial phase is located outside "dead zone" and the wind speed exceeds a certain value. As shown in Fig.7a, the time-rotating speed curve of wind turbine A at different wind speeds includes two stages, namely, ①approximately linear acceleration and ②stable equilibrium. With the increase of wind speed, the time of linear acceleration stage ① decreases and the maximum rotating speed increases significantly. As shown in Fig.7b, the starting behavior of the wind turbine B

is similar to that of the wind turbine A, when the wind speed is less than 10m/s. However, the wind turbine B presents the second starting behaviour characteristics, when the wind speed is greater than 10m/s, of which the time–rotating speed curve includes four stages in case of 10m/s, namely, ① linear acceleration, ②slow acceleration or plateau, ③rapid acceleration and ④stable equilibrium. As the wind speed increases, the time required in the first three stages is reduced, especially in stage ②.
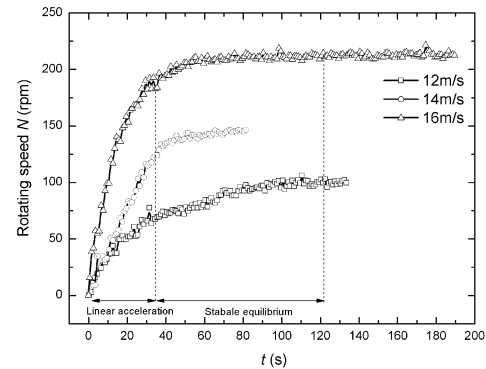
a. Wind turbine A
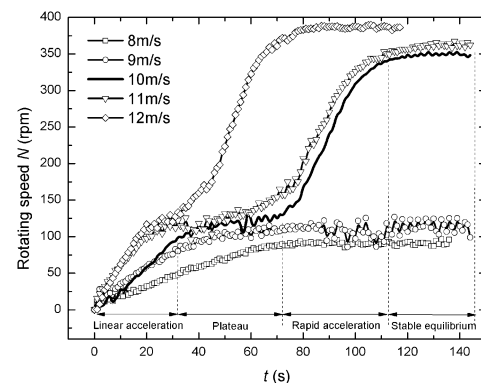
b. Wind turbine B

Fig. 7. Change curve of rotating speed of wind turbine with time.

In order to verify whether the two kinds of wind turbines are self-starting, the time-rotating speed curve in Fig.7 is converted to the time-tip speed ratio curve in Fig.8 based on the Lunt's definition of self-starting. It can be seen that the tip speed ratios for both the wind turbine A at all the test wind speeds and the wind turbine B under the wind speed less than 10m/s are less than 1, which corresponds to the starting behavior characteristic of the stages ① and ②, indicating that the wind turbine does not realize self-starting. However, the tip speed ratio of the wind turbine B at wind speed more than 10m/s exceeds 1 in stage ③, which corresponds to the starting behavior characteristics of the stages ①-④, indicating that the real self-starting is realized and the stage ③ is crucially important for distinguishment of self-starting.
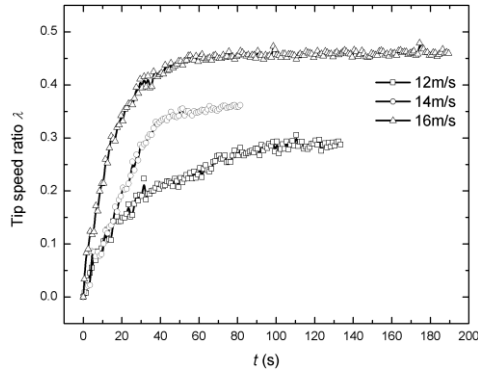
a. Wind turbine A
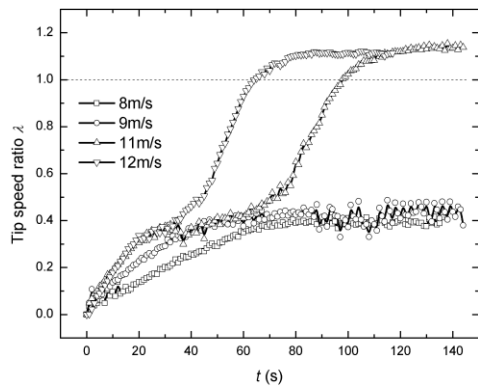
b. Wind turbine B

Fig. 8. Change curves of tip speed ratio of wind turbine with time.

4.3 Aerodynamic Torque Variation in Starting Process

In order to reveal the mechanism of the self-starting and explain the reason for two different stating bahavior characteristics, the aerodynamic torque change of the H-type wind turbine is analyzed in starting process. The aerodynamic torque M_a is indirectly obtained based on angular momentum theorem, as shown in Eq. (4). The time-angular acceleration $\dot{\omega}$ can be used to characterize aerodynamic torque due to the constant of the moment of inertia J of the wind turbine, which is derived by taking the derivation of time-rotating speed, as shown in Eq. (5).

$$M_a = \frac{dN}{dt} \frac{\pi}{30} J + M_f \qquad (4)$$

$$\dot{\omega} = \frac{dN}{dt} \frac{\pi}{30} \qquad (5)$$

where, M_f is the friction torque less than 0.03Nm, which is negligible.

Taking the wind turbine B at 8m/s and 12m/s as examples corresponding to two different starting behavior characteristics, the angular acceleration and tip speed ratio curves at these two wind speeds are derived, respectively, as shown in Fig.9.

Figure9a shows the case of 8m/s, it can be seen that there is a peak angular acceleration at initial stage, the tip speed ratio is far less than 1, and the wind turbine blade experiences large angle of incidence at most phase positions at this time. Besides, the initial rotating speed is relatively lower, resulting in low Reynolds number. The coupling effect of high angle of incidence and the low Reynolds number causes the blade to produce extremely low lift. Therefore, the initial peak acceleration is not attributed to the lift. However, the blade drag alternately acts as the driving force and the drag force at initial stage, which is larger at high angle of incidence and insensitive to the Reynolds number. Therefore, it is concluded that the initial peak angular acceleration is mainly dominated by the drag. As the tip speed ratio increases, the angular acceleration decreases sharply to relatively low value firstly, then the minimum value is obtained over a long time, because the large angle of incidence decrease finitely due to the slow increase of the tip speed ratio, resulting in slight increase of the lift, but significant decrease of the drag. The period is defined as conversion stage that the negative effect of the decreased drag outweighs the positive effect of the increased lift in the driving force. The angular acceleration is reduced to zero at the end of conversion stage, impeding further acceleration and ultimately reaching the stable equilibrium state with the tip speed ratio less than 1.
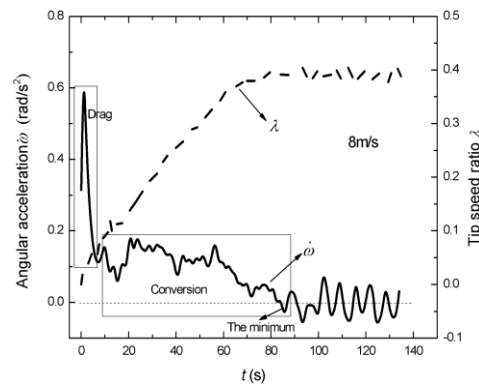
a. V=8m/s
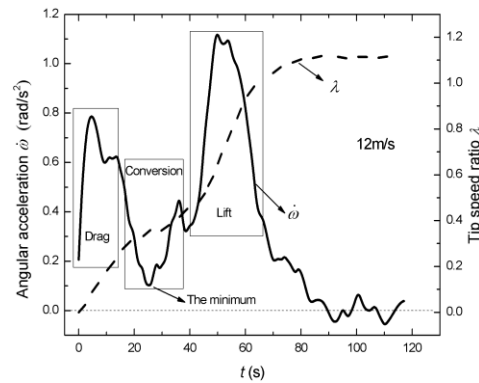
b. V=12m/s

Fig. 9. Change curves of wind turbine aerodynamic force with time during starting process.

Figure 9b shows the angular acceleration and tip speed ratio curves of the wind turbine B at 12m/s. It can be seen that the angular acceleration curve of the initial and conversion stages is similar to the case of 8m/s. However, the minimum value of the angular acceleration in the conversion stage is always greater than zero, promoting continuous acceleration of the wind turbine. As the tip speed ratio increases, the angle of incidence of the blade gradually decreases, leading to significantly increased lift as the dominated driving force and the decreased drag be mainly as barrier. The second peak angular acceleration is obtained when the lift-drag ratio is maximum. After passing the second peak, the angular acceleration drops sharply, while the tip speed ratio eventually increases to more than 1.

5. CONCLUSION

(1) Not all three-blade H-type wind turbines start from rest independently on the phase angles, based on the static torque distribution characteristics of two different H-type wind turbines. Therefore, the first challenge of self-starting to overcome is that the static torques at all phase angles are larger than the friction torque.

(2) The criterion of self-starting also needs to analyze the stating behavior characteristics in starting process. H-type wind turbine exhibits two different under the action of various wind speeds and aerodynamic shapes. The self-stating behavior characteristics are characterized by four stages, including linear acceleration①, slow acceleration②, rapid acceleration③ and stable equilibrium④ with tip speed ratio more than 1. The stage ① is mainly determined by the drag and the stage ③, ④ are dominated by the lift. The driving force conversion from the drag to lift taking place in stage ② plays an important role in self-starting, in which the minimum angular acceleration more than zero determines the wind turbine further acceleration.

REFERENCES

Arab, A.，M. Javadi, M. Anbarsooz and M. Moghiman (2017). A numerical study on the aerodynamic performance and the self-starting characteristics of a Darrieus wind turbine considering its moment of inertia. *Renewable Energy* 107, 298-311.

Asr, M. T., E. Z. Nezhad, F. Mustapha and S. Wiriadidjaja (2016). Study on start-up characteristics of h-darrieus vertical axis wind turbines comprising naca 4-digit series blade airfoils. *Energy* 112, 528-537.

Bhutta, M. M. A., N. Hayat, A. U. Farooq and Z. Ali (2012). Vertical axis wind turbine – A review of various configurations and design techniques. *Renewable and Sustainable Energy Reviews* 16(4), 1926-1939.

Biadgo, A. M., A. Simonović, D. Komarov and S. Stupar (2013). Numerical and Analytical Investigation of Vertical Axis Wind Turbine. *FME Transaction* 41 (1), 49-58.

Chua, K. L. (2002). www. Wind-turbineanalysis. netfirm.com

Dominy, R. G., P. Lunt, A. Bickerdyke and J. Dominy (2007). Self-starting capability of a Darrieus turbine. *Proceedings of the Institution of Mechanical Engineers，Part A: Journal of Power and Energy* 221(1), 111-120.

Hill, N., R. Dominy, G. Ingram and J. Dominy (2009). Darrieus turbines：The physics of self-starting. *Proceedings of the Institution of Mechanical Engineers Part A: Journal of Power & Energy* 223(1), 21-29.

Islam, M., M. R. Amin, D. S. Ting and F. Amir (2007). Aerodynamic Factors Affecting Performance of Straight-Bladed Vertical Axis Wind Turbines. *ASME 2007 International Mechanical Engineering Congress and Exposition* 47, 13-23.

Kentfield, J. A. C. (1996). The fundamentals of wind-driven water pumpers. London: Taylor & Francis.

Kirke, B. K. (1998). *Evaluation of self-starting vertical axis wind turbines for stand-alone applications.* Griffith University, Australia.

Li, Z. W. and D. X. He (2013). Reviews of fluid dynamics researches in wind energy. *Advances in Mechanics* 43(5), 472-525.

Lunt, P. A. V. (2005) An aerodynamic model for a vertical-axis wind turbine. *MEng Project Report*，School of Engineering，University of Durham，UK.

Sengupta, A. R., A. Biswas and R. Gupta (2016). Studies of some high solidity symmetrical and unsymmetrical blade H-Darrieus rotors with respect to starting characteristics，dynamic performances and flow physics in low wind streams. *Renewable Energy* 93, 536-547.

Sheldahl, R. E. and P. C. Klimas (1981). *Aerodynamic characteristics of seven symmetrical airfoil sections through 180-degree angle of attack for use in aerodynamic analysis of vertical axis wind turbines.* No. SAND-80-2114. Sandia National Labs., Albuquerque, USA.

Singh, M. A., A. Biswas and R. D. Misra (2015). Investigation of self-starting and high rotor solidity on the performance of a three S1210 blade H-type Darrieus rotor. *Renewable Energy* 76, 381-387.

Singh, R. K., M. R. Ahmed, M. A. Zullah and Y. H. Lee (2012). Design of a low Reynolds number airfoil for small horizontal axis wind turbines. *Renewable Energy* 42(1), 66-76.

Worasinchai, S. (2012). *Small Wind Turbine Starting Behaviour.* Durham theses, Durham University, UK.

Zhao, Z. Z., P. H. Pan, T. G. Wang, C. Tian, X. Liu and Y. Liu (2016) Performance Improvement of Lift Type Wind Turbine with Straight Blades Based on Interference Airflow Technology. *Journal of Mechanical Engineering* 52(22), 146-152.

Zhu, J. Y., J. M. Wang and P. Q. Liu (2017). Theoretical Analysis and Experimental Investigation of Static Torque Characteristic for H-Darrieus Wind Turbine. J*ournal of Mechanical Engineering* 53(2), 150-156.

Zuo, W. and S. H. Kang (2014). Numerical simulaiton of the aerodynamic performance of a H-type wind turbine during self-starting *Applied mechanics and materials* 529, 295-302.